Subproject B2.9

Electron Transport in Strongly Correlated Quantum Dots, Wires and Films

Principle Investigator: Peter Wölfle

CFN-Financed Scientists: Verena Koerting (E13/2, 12 months), Christine Köhler (E13/2, 12 months), Tobias Küchel (E13/2 , 2 months), Ronny Thomale (E13/2 , 3 months), Alexander Branschädel (E13/2 , 11 months)

Further Scientists: Prof. Jens Paaske (Niels Bohr Institute, U Copenhagen, Denmark), Prof. K. A. Muttalib (U Florida, Gainesville, USA), Prof. E. Abrahams (UCLA, USA), Dr. Dmitry Aristov, Dr. Holger Schmidt.

Institut für Theorie der Kondensierten Materie
Karlsruhe Institute of Technology

Institut für Nanotechnologie
Karlsruhe Institute of Technology

Electron Transport in Strongly Correlated Quantum Dots, Wires and Films

Introduction and Summary

The transport of electrons in nanostructures is strongly affected by the Coulomb interaction between electrons. A number of important effects following from there have been experimentally observed, such as the Coulomb blockade, the Kondo effect , Luttinger liquid behaviour, magnetic ordering phenomena, and more. In many cases the electron system is strongly correlated, meaning that complex many-body effects are present. In this project we developed a theoretical description of some of the situations of interest, in particular (1) nanostructures showing the Kondo effect, and (2) quantum transport in disordered ferromagnetic films.

Following a theoretical prediction in the 1980s, the Kondo effect in quantum dots has been observed as a dominant feature in the current-voltage characteristics. A Kondo effect appears whenever a quantum dot with low lying internal degrees of freedom (e.g. a spin) is coupled to reservoirs. Then, at low temperatures a Kondo resonance forms in the local density of states, which allows for resonant tunnelling through the dot and leads to a drastically enhanced conductance, up to the maximum possible. During the last funding period we developed a systematic and controlled method for calculating the conductance of a Kondo dot at bias voltages larger than the characteristic energy of the Kondo effect. Our approach makes use of the perturbative renormalization group method, generalized to out of equilibrium situations. Three new elements have to be added: (1) the renormalized Kondo coupling becomes a function of energy, (2) the renormalization group flow is cut off on the scale of the spin relaxation rate, which is growing large at finite bias, (3) in a magnetic field the spin occupation is nonthermal and is driven by the current through the dot [1]. A finite bias voltage acts to suppress the screening, and an external field coupling to the pseudospin tends to shift its effect to finite bias. In some cases the Kondo effect is initiated by the finite bias. During the present funding period, we have applied our method to a number of systems of more complex structure, with excellent success [B2.9:1-7]. A microscopic derivation of our initially semiphenomenological formulation has been given in the framework of the Functional Renormalization Group method [B2.9: 8].

In addition we have developed a theory of the spin dynamics of a Kondo impurity system [B2.9: 17], in the strong coupling, Kondo screened regime. In the generic situation of different g-factors of local spin and conduction electron spins, it is found that the electron spin resonance spectrum is characterized by a superposition of two lines, one narrow and one extremely wide.

In a second project we have successfully interpreted the transport properties of quantum films, in particular ultrathin ferromagnetic films. This work has been performed in collaboration with an experimental group at the University of Florida, Gainesville, USA. The experience gained in the past periods of the CFN in work on quantum transport theory of two-dimensional systems (see the review article [B2.9:9] formed the basis for this work. We calculated quantum corrections to the longitudinal conductivity and to the anomalous Hall conductivity, in good agreement with experimental data [B2.9:10-14].

Two invited review articles on Anderson localization in disordered media were published. One of them deals with the self-consistent theory of Anderson localization and its more recent applications to classical waves and ultracold atom systems [B2.9:15]. The other one gives a broad introduction into localization phenomena [B2.9:16]

In the time period 2006-2010, subproject B2.9 has led to 17 publications, among which are 1 article in *Nature Physics*, 3 in *Phys. Rev. Lett*., 7 in *Phys. Rev. B.*, and 3 review articles.

1. Correlation effects in quantum dots

It is well-known from quantum mechanics that the effect of interaction is strongest on a system with degenerate (or nearly degenerate) ground state. Transport measurements on nano-scale structures offer a unique possibility to probe a degenerate many-body state created, e.g. by the strong Coulomb interaction between electrons in a nanostructure. Such interaction induced behavior may be exploited to functionalize nanostructures as switches, transistors, diodes, etc. In this project we studied the behavior of a subtle many-body state at a quantum dot, the Kondo resonance state, under the influence of a finite bias voltage and a magnetic field. We find large effects on the differential conductance, and other measurable quantities, as indeed observed in experiment.

It has been proposed already in 1988 [1,2] that a quantum dot with an unpaired electron and a large on-site Coulomb repulsion will show the Kondo effect. At high energy scales the quantum dot possesses a local moment (spin ½) and its equilibrium state is twofold degenerate. The antiferromagnetic coupling J of the local spin to the conduction electron spins in the leads, as described by the Hamiltonian

$$H = \sum_{\alpha=L,R,\vec{k},\sigma} (\varepsilon_{\vec{k}} - \mu_\alpha) c^\dagger_{\alpha\vec{k}\sigma} c_{\alpha\vec{k}\sigma} - BS_z \quad + \frac{1}{2} \sum_{\alpha,\alpha'=L,R,\vec{k},\vec{k}',\sigma,\sigma'} J_{\alpha'\alpha} \vec{S} \cdot (c^\dagger_{\alpha'\vec{k}'\sigma'} \vec{\tau}_{\sigma'\sigma} c_{\alpha\vec{k}\sigma}) \ , \quad (1)$$

gives rise to logarithmic terms in perturbation theory (in J), for all observables [3]. A summation of the leading logarithmic terms, achieved in a controlled way by the perturbative renormalization group method [4], shows the emergence of a new dynamically generated energy scale, the Kondo temperature $T_K = D \exp (- 1/N(0)J)$. Here D is the half-bandwidth, $N(0) = 1/2D$ the density of states of the conduction band. At temperatures $T << T_K$ the local moment gets completely screened by the conduction electron spins, and this resonance state shows up as a narrow width ($\sim T_K$) peak at the Fermi level in the local density of states $A(\omega)$ [5].

1.1. Linear and nonlinear conductance

In the linear response regime, the conductance G of a quantum dot in the Kondo regime is completely determined by the local density of states $A(\omega)$ at the dot,

$$G = \frac{e^2}{h} \ \Gamma \int d\omega \, (-\frac{\partial f}{\partial \omega}) A(\omega) \qquad (2)$$

where $f(\omega)$ is the Fermi function and Γ is the level width.

As a function of temperature T, G exhibits scaling behaviour $G = G(T/T_K)$ and increases monotonically to $G \rightarrow 2e^2/h$, for $T \rightarrow 0$ (provided there is only negligible potential scattering, as in (1)). This is a consequence of the formation of the Kondo resonance in $A(\omega)$. It is worth noting that the simple result (2) does not necessarily hold for a more complex quantum dot with several energy levels.

We have calculated the local spectral function A(ω) in equilibrium within a self-consistent approximation resumming all two-particle vertex contributions and neglecting three-particle and higher correlation functions [5]. The result is in agreement with the numerical results obtained by Wilson's renormalization group method . Our method may be generalized to stationary nonequilibrium situations.

At finite bias voltage V >> T, the differential conductance G = dI/dV, can be calculated from the current I in perturbation theory in J [6,7]

$$G(v) = \frac{3e^2}{h}(\frac{\pi}{2} g_{LR})^2 \ \ (1 + 4 g_d \ell n \frac{D}{|eV|}) + O(g^3) \ , \tag{3}$$

where $g_{LR} = J_{LR}\, N(0)$ and $g_d = ½\ (g_{LL} + g_{RR})$ are dimensionless bare coupling constants. In the presence of a magnetic field B many more logarithmic terms appear in the current I [6,8],

$$I = \frac{e^2}{h}(\frac{\pi}{2} g_{LR})^2 \{ \sum_{\beta=0,\pm 1} (V + \beta B)(1 + 4 g_d \ell n \frac{D}{|V + \beta B|}) - M \Phi(T, V, B) \} \tag{4}$$

Here M is the local spin polarization and Φ is given by an expression somewhat similar to the first term in (4). Perturbation expressions for I have been derived since the sixties, with, however, one important difference: In these earlier works it was assumed that the local spin is in thermal equilibrium, and $M = M_{eq}$, despite the fact that at eV >> T the system is driven out of equilibrium. The corresponding change in M can amount to orders of magnitude as will be shown in the next section, and will change the current I considerably. Unlike the situation in equilibrium, where the leading logarithms in each order of perturbation theory may be easily summed up, this is not immediately possible out of equilibrium. The logarithmic terms appear in different combinations, with no obvious systematics. We will show below how they may be summed up again.

1.2. Local occupation numbers and density matrix of a correlated quantum dot in nonequilibrium

In order to calculate, e.g., the local magnetization $M = n_\uparrow - n_\downarrow$ of a S=1/2 Kondo dot, where $n_{\uparrow,\downarrow}$ are the spin occupation numbers $(n_\uparrow + n_\downarrow = 1)$, a quantum Boltzmann equation has to be solved [6,7,9]. In lowest order, it reduces to a classical rate equation.

In some cases it is not sufficient to consider only the nonequilibrium effect on the occupation numbers, since the density matrix may be nondiagonal.
The eigenstates of an isolated nanostructure may get mixed by the coupling to external leads. This effect is the stronger, the smaller the level splitting on the dot and the larger the broadening induced by the coupling to the leads is. In [B2.9:3] we describe how to calculate the nondiagonal density matrix on the nanostructure efficiently.
As a further example of the importance of the nonequilibrium occupation of the local states on the dot we consider in [B2.9:2] a lateral double-dot system in the Coulomb blockade regime with a single spin 1/2 on each dot, mutually coupled by an antiferromagnetic exchange interaction (Fig.1).

The Coulomb interaction between the dots is neglected, and hopping between the dots is not allowed. Each of the two dots is contacted by two leads.

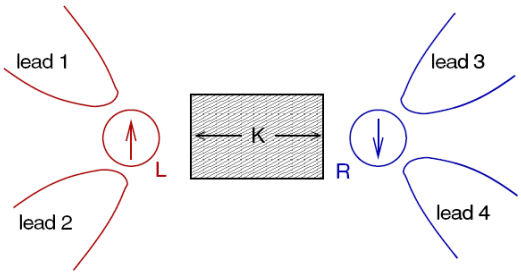

Fig. 1: Double quantum dot : Two spins ½ are coupled by exchange interaction K

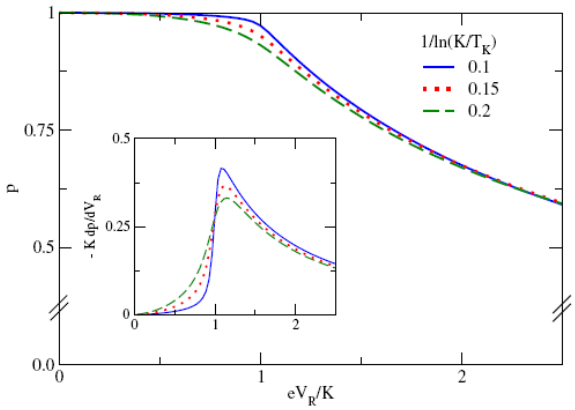

Fig. 2: Polarization $p=n_s-n_t$ (difference in occupation of singlet and triplet state) versus eV_R/K

We demonstrate that the voltage across one of the dots has a profound influence on the occupation of the triplet state (Fig.2) and the current passing through the other dot. In simple terms, this can be understood by observing that in the singlet ground state of the system transport is blocked because each tunnelling process requires a spin flip excitation into the triplet state, which costs an excitation energy J. Only when the bias voltage is large enough to provide this energy a current will flow.

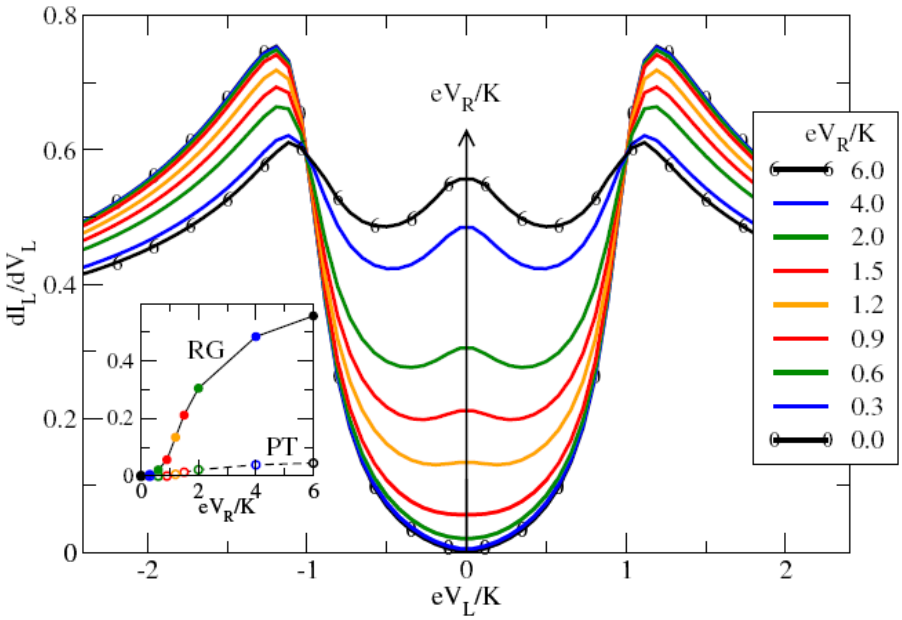

Fig. 3: Differential conductance dI_L/dV_L in units of e^2/h for fixed T/T_K= 0,1 and 1/ ln(K/T_K)= 0,2 versus eV_L/K at different values of eV_R/K. Inset: dI_L/dV_L at $V_L \rightarrow 0$ versus eV_R/K . Solid circles: perturbative RG; open circles: second order PT.

We now show that the excitation of the system into the triplet state may be effected by a separate current flowing through quantum dot 2 . Whenever that current is large enough to provide a sufficient excitation, the current through quantum dot 1 will be strongly enhanced, i.e. a

transconductance arises (Fig.3). Using poor man's scaling (see the following section), we find that the Kondo effect can lead to a strong enhancement of this transconductance.

1.3. Resumming the logarithms: Perturbative renormalization group.

The logarithmic terms in perturbation theory, e.g. in (3,4) are seen to diverge in the limits $V \to 0$, $B \to 0$, $V \to B$ and $T \to 0$. A systematic resummation of the leading logarithmic terms in perturbation theory is required, which leads to a non-diverging result. We have generalized the well-known renormalization group (RG) approach to the equilibrium Kondo problem to nonequilibrium [8,9]. Whereas in equilibrium it is sufficient to consider the renormalization of the coupling constants g under the process of removing high energy states (continuously reducing the conduction electron bandwidth 2D), in nonequilibrium one is forced to consider energy dependent coupling functions $g(\omega)$. The reason is that the coupling renormalizes in a different way for electrons with different energy ω: highly excited electrons are insensitive to low energy processes. In equilibrium one is usually interested only in electrons at the Fermi energy ($\omega = 0$) and hence it is sufficient to consider only the coupling constant $g(\omega = 0)$. Exceptions are properties of excited electrons, such as the conduction electron T-matrix at energies $\omega >> T_K$. In nonequilibrium, by contrast, even at $T = 0$ electrons in a finite energy window $|\omega| < eV/2$ contribute, so that for $eV > T_K$ it is necessary to know the full energy dependence of $g(\omega)$. For the double dot system considered above the RG equations in one loop order (see Fig. 4) read [B2.9:2]:

$$\begin{aligned}\frac{\partial g_{\rm tt}^{nm}(\omega)}{\partial \ln D} &= -\frac{1}{2}\sum_l \{g_{st}^{lm}(\mu_l) g_{ts}^{nl}(\mu_l - K)\Theta_{\omega-\mu_l+K} \\ &+ g_{st}^{nl}(\mu_l + K) g_{ts}^{lm}(\mu_l)\Theta_{\omega-\mu_l-K} \\ &+ 2 g_{\rm tt}^{lm}(\mu_l) g_{\rm tt}^{nl}(\mu_l)\Theta_{\omega-\mu_l}\},\end{aligned} \tag{5}$$

$$\begin{aligned}\frac{\partial g_{ts}^{nm}(\omega)}{\partial \ln D} &= -\sum_l \{g_{ts}^{lm}(\mu_l) g_{\rm tt}^{nl}(\mu_l)\Theta_{\omega-\mu_l} \\ &+ g_{\rm ts}^{nl}(\mu_l - K) g_{\rm tt}^{lm}(\mu_l)\Theta_{\omega-\mu_l+K}\},\end{aligned}$$

Here $g_{tt}(\omega)$ and $g_{ts}(\omega)$ are the triplet to triplet and triplet to singlet coupling functions and (n,m) are the lead indices and Θ_ω are modified step functions (see below).

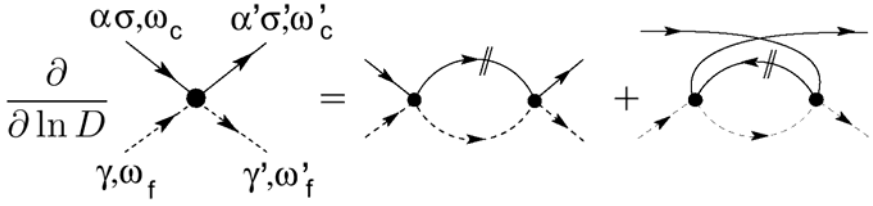

Fig. 4: Diagrammatic form of the RG equation (5). The strokes symbolize derivatives with respect to ln D.

1.4. Destruction of Kondo correlations by relaxation effects out of equilibrium.

The RG equations (6) are incomplete in that the effect of inelastic processes on the coherence of the rearrangement processes in the Fermi sea following a spin flip is not taken into account yet. We have obtained a first indication of the prominent role of inelastic processes induced by a finite current through the Kondo dot in the framework of a conserving, self-consistent theory on the level of the non-crossing approximation (NCA) [10]. There we found that the broadening of the local spin levels and vertex corrections lead to a suppression of the Kondo effect: the formation of the infrared singularity leading to the formation of the Kondo resonance state is interrupted by inelastic processes on a frequency scale $\Gamma >> T_k$, provided $eV >> T_k$. Hence the Kondo effect never fully develops under these conditions. More recently we have succeeded in showing explicitly in perturbation theory that the Kondo logarithms are cut-off by a relaxation rate Γ, which is given by either the transverse or the longitudinal spin relaxation rate [11]. While in equilibrium this relaxation rate for $T >> T_k$ is given by the Korringa law, $\Gamma_{eq} \sim g_0^2 T$, and may be safely neglected, in nonequilibrium $\Gamma \sim g_0^2 V >> \Gamma_{eq}$, if $eV >> T$. Beyond perturbation theory Γ may be calculated from the golden rule expression with, however, g_o replaced by the renormalized $g(\omega)$.

This has important consequences for the RG flow: the flow stops at $D \sim \Gamma$. It turns out that the renormalized coupling functions at this scale obey $g(D=\Gamma) << 1$, provided the condition $g_{LR}/\max(g_{LL}, g_{RR}) >> \sqrt{T_k/V}$ is satisfied. It is in fact difficult to violate this condition. In practical terms we have implemented the cutoff by replacing the step functions in (5) by $\theta_\Gamma(\omega) = \theta(D - \sqrt{\omega^2 + \Gamma^2})$.

1.5. Physical observables and comparison with experiment

In one-loop approximation we may calculate physical observables from the lowest order expressions, with the bare coupling constants substituted by the renormalized ones. We thus find for the current in the case of the double dot problem considered above [B2.9:2]

$$I_L(V) = \frac{\pi^2}{2}\frac{e}{h}\sum_{\gamma\gamma'} n_\gamma \mathbf{T}_{L;\gamma\gamma'} \cdot \mathbf{T}_{L;\gamma'\gamma} \int_{-\infty}^{\infty} d\omega g^{21}_{\gamma\gamma'}(\omega) \times g^{12}_{\gamma'\gamma}(\omega - \omega_{\gamma'\gamma})[F^{12}_{\gamma'\gamma}(\omega) - F^{21}_{\gamma'\gamma}(\omega)], \tag{6}$$

where **T** is a vector of 4x4 matrices describing transitions between the four dot levels in the singlet-triplet representation and F are nonequilibrium occupation numbers of the lead electrons. Similarly, the local occupation numbers are calculated from the rate equation with renormalized couplings. The results are shown in Figs. 2 and 3.

The one-loop approximation is correct to lowest order in the small parameters $1/\ell n(V/T_k)$ or $1/\ell n(B/T_k)$. Thus, in order for this theory to be applicable we need large ratios of B/T_k, V/T_k. The

perturbative RG approach to nonequilibrium transport phenomena involving the Kondo effect is widely applicable and allows a systematic and controlled calculation of any observable .

1.6 Nonequilibrium transport at a dissipative quantum phase transition

We investigated the nonequilibrium transport near a quantum phase transition in a generic and relatively simple model, the dissipative resonant level model, that has many applications for nanosystems [B2.9:6]. We formulated a rigorous mapping and applied a controlled frequency-dependent renormalization group approach to compute the nonequilibrium current in the presence of a finite bias voltage V and a finite temperature T. For V → 0, we find that the conductance has its well-known equilibrium form, while it displays a distinct nonequilibrium profile at finite voltage. We consider the following Hamiltonian, describing a conduction band coupled to a local level. The level energy is subject to quantum fluctuations created by a bosonic bath:

$$H = \sum_{k,i=1,2} [\epsilon(k) - \mu_i] c_{ki}^\dagger c_{ki} + t_i c_{ki}^\dagger d + \text{H.c.}$$
$$+ \sum_r \lambda_r (d^\dagger d - 1/2)(b_r + b_r^\dagger) + \sum_r \omega_r b_r^\dagger b_r,$$

The bath is characterized by a spectral function

$$J(\omega) = \sum_r \lambda_r^2 \delta(\omega - \omega_r) = \alpha\omega$$

At sufficiently large dissipation parameter α the electron at the local level gets localized. The transition from localized to delocalized behaviour is of the Kosterlitz-Thouless type. The model may be mapped on to an anisotropic Kondo model, with exchange couplings $g^{\perp}=t$ and $g^{\parallel}=1-\alpha$. The phase diagram has the form

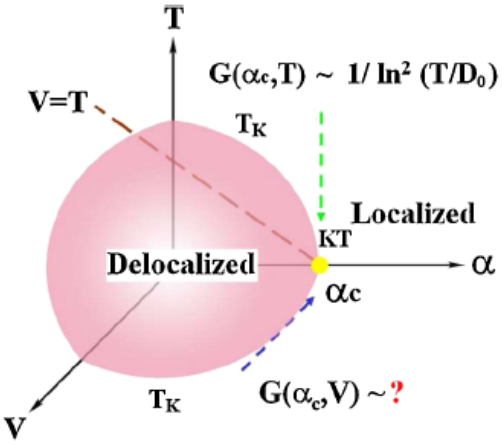

Fig. 5 : Phase diagram of the dissipative resonance level model in the temperature-voltage-dissipation parameter space.

Using the perturbative renormalization group method described above we have calculated the conductance. We find scaling behaviour in the scaled voltage variable V/T*, where the characteristic temperature T* is defined by

$$T^* = D_0 e^{-\pi/\sqrt{g_z^2 - g_\perp^2}}$$

The resulting conductance in the localized phase is shown in Fig. 6:

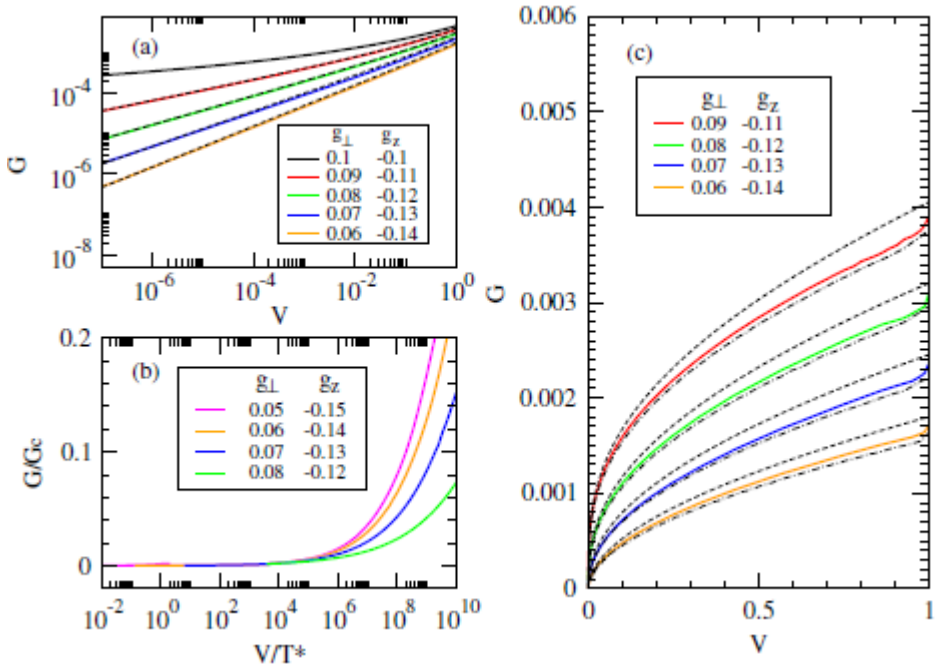

Fig. 6: (a) G(V) at low bias follows the equilibrium scaling form (dashed lines); (b) The normalized conductance G(V)/Gc is a function of V/T* up to voltages of order band width; (c) At large bias voltages the conductance is distinctly different from the equilibrium form (dashed lines). An analytical approximation captures the behavior well (dashed-dotted lines).

As a further example of a system characterized by two different ground states we considered Kondo dot coupled to Luttinger liquid leads [B2.9:7]. The interaction in the leads is characterized by the parameter K, with K=1 in the noninteracting limit. In the regime ½<K<1 the system scales to the usual one-channel Kondo fixed point. At K<½ one finds that the growth of the interlead coupling under RG is slowed down such that a two-channel Kondo fixed point is stabilized. The corresponding signatures in the conductance have been calculated in [B2.9:7].

1.7 Nonequilibrium Singlet-Triplet Kondo effect in a Carbon Nanotube Quantum Dot

A conducting carbon nanotube may be contacted to form a quantum dot (Fig. 7). The electronic structure of carbon nanotubes is characterized by a series of groups of two almost degenerate orbitals, which are both spin doublets (the spin-orbit interaction may be neglected in this context). In the standard plot of conductance versus gate voltage and bias voltage, the Coulomb diamonds show a corresponding fourfold periodicity [B2.9:1]. The diamonds assigned to N=1,3 electrons occupying the highest group of levels display a zero bias anomaly signalling the Kondo effect. By contrast, in the case N=0,2 electrons there is no zero bias anomaly. Instead, in the the N=2 case, one finds Kondo-like peaks at finite bias V, showing logarithmic growth for decreasing temperature. In a finite magnetic field the peak is found to split into three peaks [B2.9:1]. This may be understood qualitatively by observing that there are excited states where one electron is promoted from the lower level to the upper level, the two electrons forming a spin S=1 triplet state. That local spin S=1 may undergo a Kondo effect, and it will split into the three substates in a magnetic field .

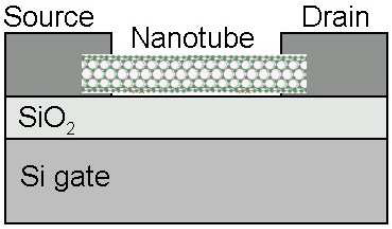

Fig. 7: Carbon nanotube quantum dot studied in [B2.9:1].

In our theoretical model description of the system we started from a corresponding Anderson model. Using a Schrieffer-Wolff type transformation the Anderson model was mapped onto a Kondo model featuring the spin S=1 operator exchange coupled to the conduction electron spin and spin-tunneling operators, as well as nonmagnetic transition operators describing transitions between the two orbitals. From the corresponding nonequilibrium RG equation we determined the renormalized coupling functions, which show sizeable enhancements at energies for which spin flip processes can take place (see Fig. 8).

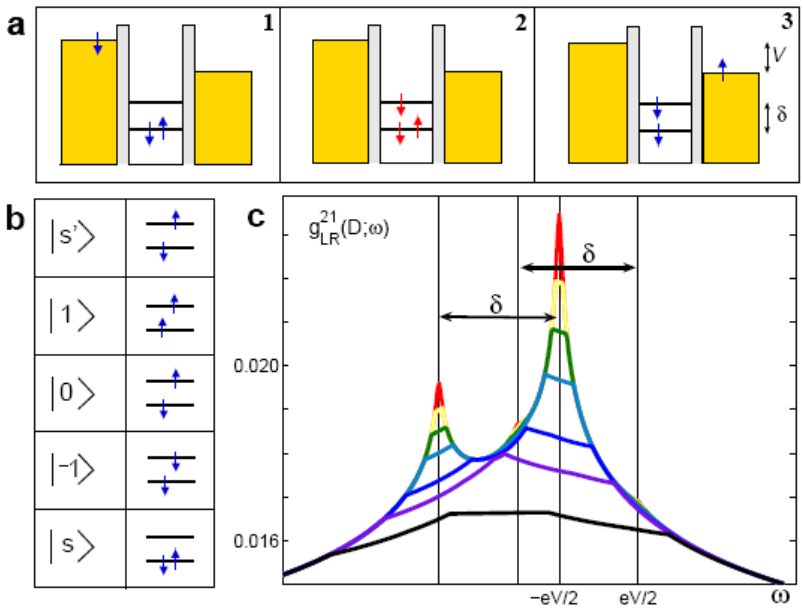

Fig. 8: Schematic of the inelastic spin-exchange underlying the Kondo effect.
a, Illustration of the cotunneling mechanism giving rise to the effective exchange-interaction in the Kondo model. Note that the virtual intermediate state (red spins) in panel 2 is suppressed by a large energy-denominator of the order of the electrostatic charging energy of the nanotube. b, Schematic of the five different low-energy states retained in the effective Kondo-model: $|s\rangle$ is the singlet ground-state, $|m\rangle$ (m=1,2,3) are the triplet components with excitation energy ± ¡ *J* ¼ ± and $|s'\rangle$ is the corresponding excited singlet state. Renormalized dimensionless exchange-coupling vs. incoming conduction electron energy ω, measuring the amplitude for exchange-tunneling from right to left lead while de-exciting an electron on the nanotube from orbital 2 to 1. Different colours encode the different stages of the RG-flow as the bandwidth is reduced from D_0 (black) to zero (red).

Having determined the renormalized coupling functions, the electrical current is finally calculated from the golden rule expression:

$$I = \frac{2\pi e}{\hbar}\int_{-\infty}^{\infty} d\omega \sum_{\substack{\sigma,\sigma'=\uparrow,\downarrow \\ \gamma,\gamma'=s,-1,0,1,s'}} |g^{\gamma';\gamma}_{R,\sigma';L,\sigma}(\omega)|^2 f(\omega-\mu_L)(1-f(\omega+\varepsilon_\gamma-\varepsilon_{\gamma'}-\mu_R))n_\gamma - (L\leftrightarrow R)$$

where $L=R=\pm eV/2$ denotes the two different chemical potentials, n_γ are the nonequilibrium occupation numbers of the five impurity states and g is the renormalized exchange-tunneling amplitude for transferring a conduction electron from left to right lead and changing its spin from σ to σ' , while switching the impurity-state from γ to γ'. The resulting differential conductance is shown in Fig.9 . The agreement with the data is seen to be quite satisfactory.

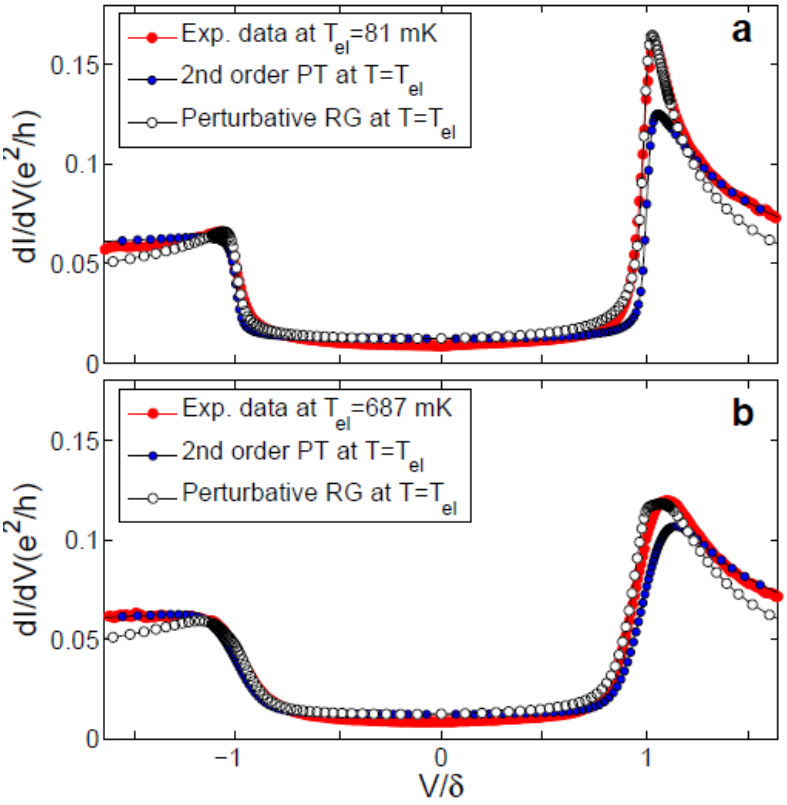

Fig.9 : Fitting the nonlinear conductance by perturbative RG calculation. a: Experimental data (red dots) at the lowest temperature, fitted by the perturbative RG calculation (white dots) with t_{L1}; t_{L2}; t_{R1}; t_{R2} = 0,023; 0,030; 0,105; 0,077 $\sqrt{E_c/v_F}$
and $T = T_{el}$ = 81 mK. We use $J = 0$ and an arbitrary bandwidth, D_0 = 1 eV, larger than all other energy-scales. From the bias at which dI/dV vs. V has maximum slope, we read off δ = 1,525 meV. The blue curve represents simple cotunneling, i.e. second order perturbation theory (PT) with tunneling-amplitudes t_i fitted to the data at T = 687 mK (see panel b).
b: Comparing to the data (red and white dots) at the highest temperatures, using same parameters as in panel a, but with $T = T_{el}$ = 687 mK. The blue curve represents the best fit of second order perturbation theory with T = 687 mK.

References

1.8 Spin dynamics of a quantum dot in the Kondo regime

As discussed above, at temperatures T below the dynamically generated energy scale T_K, the Kondo temperature, the exchange interaction with the conduction electron spins causes a local spin 1/2 to be fully screened. This behavior should be noticeable in the temperature dependence of the spin dynamics of the system, as probed by electron-spin resonance _ESR_. In fact, the local spin resonance in dilute Kondo compounds at $T>> T_K$ had been observed even before the Kondo effect was understood. Afterward there were a number of systematic experimental investigations and perturbative calculations for the ESR at $T>> T_K$ in dilute Kondo systems [12].
At low temperatures $T<< T_K$, on the other hand, neutron scattering studies revealed the existence of a broad spin excitation peak of width T_K , interpreted as the Kondo bound state [13]. Within the isotropic *s-d* exchange (Kondo) model the total spin is conserved. Therefore, in the limit of equal g factors of local moments and conduction-electron spins, one expects a single spin-resonance line at all temperatures, only broadened by spin-lattice relaxation. As we have shown [B2.9:17], in this limit the weight of the broad local spin resonance tends to zero.
We start from the bare Anderson model Hamiltonian, describing the hybridization of a local level with the conduction band. Two electrons of opposite spin on the local level experience a strong Coulomb repulsion U, which leads to essentially single occupancy of the level and consequently a local moment.
In the framework of Fermi-liquid theory, at low temperatures $T<< T_K$, the interaction U has two major consequences: (i) it gives rise to a molecular field renormalizing the collective response of the system and (ii) it leads to a finite lifetime of quasiparticles. However, the quasiparticle relaxation rate is limited by the available phase space and vanishes quadratically as the excitation energy goes to zero. Therefore, at temperatures $T<< T_K$ the Landau quasiparticles are well defined. The quasiparticle decay contributes to the spin-relaxation rate. As we show, the local-moment relaxation is governed by rapid spin flips on the frequency scale of T_K , occurring as part of the many-body resonance. Then at temperatures $T<< T_K$ we may neglect the additional relaxation caused by the quasiparticle decay. Within Fermi liquid theory, we have calculated the dynamical spin susceptibility for the realistic case of different g-factors of local moment and conduction electron spins [B2.9:17]. The ESR spectrum is found to be characterized by a narrow peak of the width of the spin-lattice relaxation rate, on top of a broad peak of width T_K , their relative weight depending on the ratio of g-factors.
These results on the Kondo impurity model have consequences for Kondo lattice systems as well. In this framework one may interpret the recently discovered narrow spin resonance lines in certain heavy fermion systems in a semi-quantitative way. The crucial observation is, that the broad peak contributed to the spin resonance by the local moments gets absorbed into the heavy quasiparticle band structure. The resonance line gets broadened only by quasiparticle scattering and by the spin-lattice relaxation rate, both strongly reduced by ferromagnetic correlations [B2.9:17].

2. Quantum Transport in ultrathin ferromagnetic films

Quantum corrections to the conductivity of disordered metallic films have been the subject of numerous investigations. One finds two types of corrections, a weak localization correction and an interaction induced (Altshuler-Aronov) correction both proportional to ln(T) . A very interesting new situation arises in ferromagnetic films due to the presence of spin wave excitations. In ferromagnetic films one encounters the socalled anomalous Hall effect, i.e. a Hall effect caused by the ferromagnetically aligned magnetic moments [for a review see B2.9:10]. On the basis of symmetry arguments and by direct calculations we have shown that there is no interactiion induced quantum correction to the Hall conductivity [B2.9:12, 14].

In a series of *in situ* transport measurements on ultrathin (< 100 A thick) polycrystalline Fe films as a function of temperature and magnetic field quantum corrections have been observed for a wide range of disorder strengths [B2.9:11]. For sheet resistances R_{xx} less than 3kΩ , one finds a logarithmic temperature dependence of the anomalous Hall conductivity R_{xy}, which is shown for the first time to be due to a universal scale dependent weak-localization correction within the skew-scattering model. This is possible because in a ferromagnet the dominant contribution to phase relaxation comes from scattering of electrons by spin waves [B2.9:14], which turns out to be more effective than the usual Coulomb interaction mechanism. For higher sheet resistance, granularity becomes important and the break down of universal behavior becomes manifest as the prefactors of the ln$T$ correction term to R_{xx} and R_{xy} decrease at different rates with increasing disorder.
In a more recent study of transport in ferromagnetic Gadolinium films *in situ* magneto-transport measurements were performed on a series of thin films with thickness d < 135A [B2.9:13] . For sheet resistances R_0 < 3kΩ, and temperatures T < 30K, we observe a linear temperature dependence of the conductivity in addition to the logarithmic temperature dependence expected from well-known quantum corrections in two dimensions. We show that such a linear T-dependence can arise from a spin-wave mediated Altshuler-Aronov type correction [B2.9:13]. In Fig. 8 conductivity data are plotted versus temperature on a logarithmic scale. These data may be fitted to a function

$$\sigma(T)= P_1+P_2\ln(T/T_0)+P_3(T/T_0)^p \qquad (7)$$

The resulting values of the parameters as a function of disorder are shown in Fig.11 . A linear power law contribution, as given by the Altshuler-Aronov correction induced by the effective spin-wave mediated electron-electron interaction is clearly visible.

At even stronger disorder one finds scaling behaviour of the conductivity characterized by universal fractional exponents. This observation signals that the system is in the scaling regime at the metal-insulator transition in three dimensions. These films are indeed effectively threedimensional at strong disorder and not too low temperature (regime 5K to 50 K), because the dephasing length is sufficiently short (as explained above). Work in this direction is in progress.

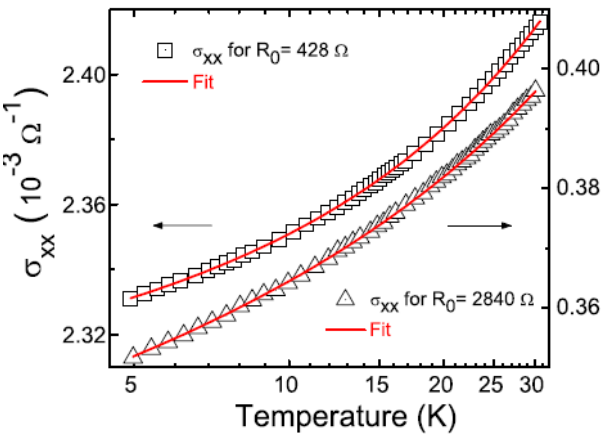

Fig. 10: Longitudinal conductivity of Gadolinium films versus temperature for two samples with resistances R0 at T=5K.

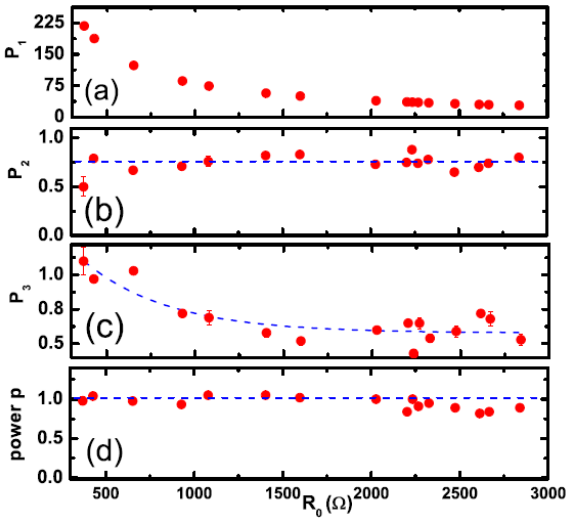

Fig. 11: Parameters determined from a fit of the data to Eq. (7) .

References

- own work with complete titles -

[1] T. Ng and P.A. Lee, Phys. Rev. Lett. **61**, 1768 (1988).

[2] L. Glazman and M. Raikh, JETP Letters **47,** 452 (1988).

[3] A.C. Hewson, *The Kondo problem to heavy fermions,* (Cambridge University Press, 1993).

[4] P.W. Anderson, J. Phys. C **3**, 2436 (1970)

[5] J. Kroha and P. Wölfle, *Conserving diagrammatic approximations for quantum impurity models: NCA and CTMA*, In: Festschrift "40 years Kondo effect", J. Phys. Soc. Jpn. **74**, 16 (2005).

[6] J. Paaske, A. Rosch and P. Wölfle, *Nonequilibrium transport through a Kondo dot in a magnetic field: Perturbation theory,* Phys. Rev. B **69**, 155330 (2004).

[7] P. Wölfle, A. Rosch, J. Paaske, and J. Kroha, *Nonequilibrium transport through a Kondo dot in a magnetic field,* Adv. in Solid State Physics **42**, 175 (Springer, 2002).

[8] A. .Rosch, J. Paaske, J. Kroha, and P. Wölfle, *The Kondo effect in nonequilibrium quantum dots: Perturbative renormalization group*, In: Festschrift "40 years Kondo effect", J. Phys. Soc. Jpn. **74**, 118 (2005).

[9] A. Rosch, J. Paaske, J. Kroha and P. Wölfle, *Nonequilibrium transport through a Kondo dot in a magnetic field: perturbation theory and poor man's scaling*, Phys. Rev. Lett. **90**, 76804 (2003).

[10] A. Rosch, J. Kroha and P. Wölfle, *The Kondo effect in quantum dots at high voltage: Universality and scaling,* Phys. Rev. Lett. **87**, 156802 (2001).

[11] J. Paaske, A. Rosch, J. Kroha and P. Wölfle, *Nonequilibrium transport through a Kondo dot: decoherence effects*, Phys. Rev. **B 70,** 155301 (2004).

[12] W. Brenig, W. Götze, and P. Wölfle, *Spin relaxation and transport in local-moment systems,* Phys. Rev. B **2**, 4533 (1970)

[13] U. Walter, E. Holland-Moritz, and Z. Fisk, Phys. Rev. B **43**, 320 (1991).

[14] A. Langenfeld and P. Wölfle, *Absence of quantum corrections to the anomalous Hall conductivity,* Phys. Rev. Lett. **67**, 739 (1991).